Journal of Magnetic Resonance **148,** 257–266 (2001)
doi:10.1006/jmre.2000.2257, available online at http://www.idealibrary.com on IDEAL®

Computer Simulation of the Spin-Echo Spatial Distribution in the Case of Restricted Self-Diffusion

Andrej Duh,* Aleš Mohorič,† and Janez Stepišnik†,‡

*Faculty of Electrical Engineering and Computer Science, Institute of Mathematics and Physics, University of Maribor, Smetanova 17, 2000 Maribor, Slovenia; †Faculty of Mathematics and Physics, Physics Department, University of Ljubljana, Jadranska 19, 1000 Ljubljana; and ‡Institute Josef Stefan, Jamova 39, 1000 Ljubljana, Slovenia

Received March 24, 2000; revised September 21, 2000

This article concerns the question of a proper stochastic treatment of the spin-echo self-diffusion attenuation of confined particles that arises when short gradient pulse approximation fails. Diffusion is numerically simulated as a succession of random steps when motion is restricted between two perfectly reflecting parallel planes. With the magnetic field gradient perpendicular to the plane boundaries, the spatial distribution of the spin-echo signal is calculated from the simulated trajectories. The diffusion propagator approach (Callaghan, "Principles of Nuclear Magnetic Resonance Microscopy," Oxford Univ. Press, Oxford, 1991), which is just the same as the evaluation of the spin-echo attenuation by the method of cumulant expansion in the Gaussian approximation, with Einstein's approximation of the velocity correlation function (VCF) (delta function), agrees with the results of simulation only for the particle displacements that are much smaller than the size of the confinement. A strong deviation from the results of the simulation appears when the bouncing rate from the boundaries increases at intermediate and long gradient sequences. A better fit, at least for intermediate particle displacements, was obtained by replacing the VCF with the Oppenheim–Mazur solution of the Langevin equation (Oppenheim and Mazur, *Physica* 30, 1833–1845, 1964), which is modified in a way to allow for spatial dependence of particle displacements. Clearly, interplay of the correlation dynamics and the boundary conditions is taking place for large diffusion displacements. However, the deviation at long times demonstrates a deficiency of the Gaussian approximation for the spin echo of diffusion inside entirely closed pores. Here, the cumulants higher than the second one might not be negligible. The results are compared with the experiments on the edge enhancement by magnetic resonance imaging of a pore.

Key Words: **molecular velocity correlation; nuclear magnetic resonance; spin-echo; restricted; confined self-diffusion; spin spatial coherence; porous system.**

1. INTRODUCTION

The advance of NMR measurement techniques, such as spin-echo and magnetic resonance microscopy, enables a detailed study of self-diffusion in fluids confined in a porous medium. Here the influence of boundary restriction has important implications on molecular motion and fluid transport. Different theoretic approaches have been developed to describe the spin-echo attenuation of restricted diffusion. Two of these are notable in being distinct in performing the average of the spin phase to get the spin-echo attenuation. These are the propagator method (*1, 3, 4*) and the method of the cumulant expansion in the Gaussian approximation (*5–8*). The purpose of this paper is to test these methods with the results of computer simulation of the spin-echo signal distribution in an entirely closed pore, as well as with the previously published results of simulation (*9*) and experiments on magnetic resonance imaging (MRI) diffusion edge enhancement (*10*).

Although the use of magnetic field gradients to detect the translational displacement of molecules via the precession of their atomic nuclear spins dates back into the early days of NMR (*11*), some obscured problems concerning measurement of diffusion in a system, for which restriction to motion causes a deviation from the Fickian behavior, still remain open. The Bloch equation with the diffusion term (Bloch–Torrey equation) (*12*) has been introduced to describe the spin-echo attenuation in a bulk of homogeneous liquid, while Stejskal and Tanner (*13*) initiated the methodology and theory of the pulsed gradient spin echo (PGSE, Fig. 1) for measurements of restricted molecular self-diffusion. The self-diffusion coefficient reduces due to molecular collisions with barriers when the time interval between the gradient pulses is long enough. The PGSE method has been extensively investigated. A number of studies consider various problems of molecular self-diffusion in a bounded region, using the diffusion propagator from the familiar Einstein's formula (*14*) for Brownian motion (leading to Fick's diffusion equation) to average out the motional spin phase fluctuations. Among others, Callaghan has found the diffusive diffraction of the spin-echo signal as a function of the gradient magnitude (*1, 4, 15*). The method provides information about the microstructure of a heterogeneous system directly from the PGSE measurements. Although spin phase averaging with Fick's diffusion propagator was able to disclose new effects, its application is limited to the spin-echo sequence consisting of two short gradient pulses (*16*).

Fick's diffusion equation, which is commonly used to derive

1090-7807/01 $35.00

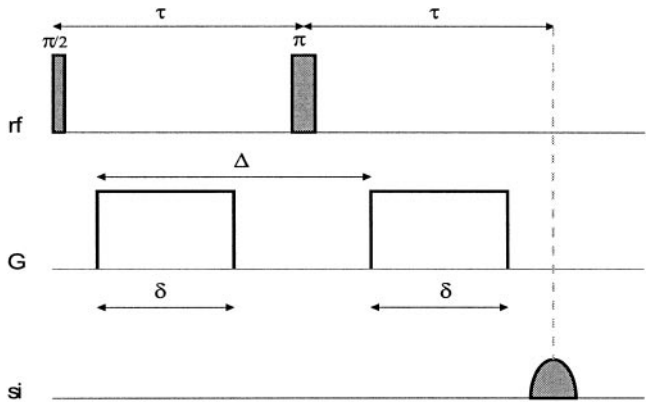

FIG. 1. The combination of RF and gradient pulses for a PGSE experiment. The symbol δ represents the length of the gradient pulse: Δ is the time between two successive gradient pulses. Spin-echo peak appears after time 2τ from the start of the experiment.

the propagator, is adequate in describing the underlying process of spin phase fluctuations only after some information is lost by limiting the precision of temporal and spatial measurements (*7, 18*). The equation might describe a process on a cruder level than a process of diffusion in a small restricted region allows for. This means that the application of the propagator method to the restricted diffusion, when the particles' mean displacement is comparable to the size of pore, is quite questionable.

In parallel, the method that handles the spin phase average with the use of cumulant expansion in the Gaussian approximation (*19, 20*) has been introduced. This method links the single-particle velocity correlation function (VCF), which contains details of motion and interaction on the molecular level, to the spin-echo variables. It enables one to observe the world of microscopic motion through the window, whose opening is determined by the form of the gradient pulse sequence (*21, 22*). Properly shaped sequences become a tool to acquire information, not only about macroscopic flow and diffusion, but also about the motion on a molecular level (*23, 24*). For the spin-echo attenuation caused by restricted diffusion, this approach provides a new understanding of the phenomena (*6, 7, 25*).

Both methods give an identical result for the free diffusion described by Einstein's formula for the VCF (*14*), but the restricted diffusion is an example where a difference occurs (*6, 7*). The experiments (*25*) verify that the cumulant expansion in the Gaussian approximation properly describes the spin-echo diffusion measurements in a medium of interconnected pores when a long or modulated gradient sequence is applied. However, it has been also confirmed (*6*) that this method predicts less distinctive pits of the diffusive diffraction pattern (*6*) in comparison to the results obtained by the propagator method (*15*) for the diffusion in a system of completely closed pores.

The aim of this paper is to set the measure for comparing these theoretical approaches with the results of numerical simulation and with the results of previous experiments on the edge enhancement in the magnetic resonance imaging. Instead of simulating the mean spin response from the bulk of sample, as has been shown in many references (*15, 17, 26–28*) we deal here with the spatial distribution of the spin-echo signal in a small compartment. In Ref. (*9*), the signal distribution has been studied by the use of the impulse-propagator method based on the matrix multiplication for long gradient pulses. This method numerically overcomes the short pulse limit of the propagator approach, but for long evolution time the spectral distortion appears which unreality broadens the image far beyond the edge of the sample. Although it provides a similar signal intensity compared to our results, here a simulation method is needed that provides distribution with higher accuracy for a precise comparison with theories.

The simulated spatial distribution of the spin-echo signal represents an equivalent of the MR image, if assuming the data acquisition interval to be short enough, with respect to the inverse rate of the diffusion attenuation. Otherwise, the spin-echo attenuation within the readout interval cannot be neglected. It might unnecessarily complicate the calculations. The results of simulation can also be compared with the results of MRI diffusive edge enhancement obtained in Refs. (*10, 29–32*).

2. THEORY

2.1. The Mean of the Spin Phase Fluctuation

Whenever a nonuniform magnetic field is used in NMR to encode the spin magnetization for motion rather than position, it is appropriate to refocus any spin phase shift, due to absolute spin position, in a spin echo. This means that the time integral of the effective gradient, $\mathbf{G}(t)$, is zero. A small perturbation of the spin phase, due to molecular displacements in the magnetic field, can be written as $\theta(2\tau) = \gamma \int_0^{2\tau} \mathbf{G}(t) \cdot \mathbf{r}(t)dt = -\int_0^{2\tau} \mathbf{F}(t) \cdot \mathbf{v}(t)dt$. Here $\mathbf{F}(t) = \gamma \int_0^t \mathbf{G}(t')dt'$, 2τ is the time of the phase refocusing, $\mathbf{r}(t)$ is the instantaneous position of the particle, and $\mathbf{v}(t)$ is its velocity. Since the detected signal arises from the induction of immense number of spins ($\gg 10^6$), one does not detect the frequency fluctuations of individual spin but rather a coherent superposition of signals induced by this large number of spins. Regarding their location in a nonuniform magnetic field, particularly in MRI, one can distinguish groups of spins according to their precessional frequency at the time 2τ. For such grouping, the averages within the subensembles have to be performed. Thus, the spin-echo signal peak can be written as (*7*)

$$E(2\tau) = \sum_j E_{jo} \langle e^{-i \int_0^{2\tau} \mathbf{F}_j(t) \cdot \mathbf{v}_j(t) dt} \rangle. \qquad [1]$$

Here the summation is taken over the subensembles of spins and E_{jo} is the normalized amplitude of the jth subensemble. $\langle \ldots \rangle$ denotes the ensemble average over the motion of particles

in the jth subensemble. $\mathbf{v}(t)$ can be considered a stochastic variable and the average can be treated within the frame of the theory of stochastic process. The mean of spin phase fluctuations is commonly worked out with the use of the diffusion propagator. The method has been introduced for molecular transport in microporous crystallites (*3*), where Fick's propagator for the free diffusion was used as an effective averaged diffusion propagator to describe the diffusion in heterogeneous systems. Despite the fact that the propagator for unbounded diffusion could have a limited validity when boundaries restrict molecular motion, it provides a satisfactory explanation of diffusion measurements in confinements. A number of exact solutions for the propagator in different geometries are available by solving Fick's law using the standard eigenmode expansion (*33*).

Since the form of Eq. [1] is like a characteristic function of a stochastic process (*34*), one can employ the cumulant expansion method known from the theory of probability to calculate the mean of the spin phase. According to general theorems of statistical physics, the characteristic function of a stochastic process exists, even if the propagator does not (*18, 35*). This means that a stochastic process is fully described either by the probability distribution function, i.e., the propagator, or by the correlation functions. The characteristic function generates cumulants, i.e., the combination of moments, which are the multiple integrals of the correlation functions. In the parlance of NMR, this means that evaluation of the spin phase average can be justified either with the propagator method, if we know the distribution function, or with the cumulant expansion, when the moments are known. Exact distribution function or all correlation functions are hardly ever available and the problem can only be handled with approximations. The cumulant expansion method in the Gaussian approximation allows us to assume that the cumulants higher than the second can be neglected. Thus, the characteristic function is defined only by the average $\langle \mathbf{v}(t)\rangle$ and the second moment $\langle \mathbf{v}(t_1)\mathbf{v}(t_2)\rangle$. Thus the cumulant expansion of the spin phase (which is like a characteristic function, Eq. [1]) provides

$$\left\langle e^{-i\int_0^{2\tau}\mathbf{F}(t)\cdot\mathbf{v}(t)dt}\right\rangle = e^{-i\int_0^{2\tau}\mathbf{F}(t)\cdot\langle\mathbf{v}(t)\rangle dt} \times e^{-(1/2)\int_0^{2\tau}dt_1\int_0^{2\tau}dt_2\mathbf{F}(t_1)\cdot\langle\mathbf{v}(t_1)\mathbf{v}(t_2)\rangle_c\mathbf{F}(t_2)}. \quad [2]$$

Here the subscript c in $\langle\ldots\rangle_c$ means the cumulant combination of the first- and the second-order moments (*34*) ($\langle ab\rangle_c = \langle ab\rangle - \langle a\rangle\langle b\rangle$).

2.2. Spin-Echo Distribution in a Pore

In porous media of closely packed polystyrene beads, the measurement of restricted diffusion by the modulated gradient spin-echo method (*25*) confirms the anticipated dependence of spin-echo attenuation on time, gradient strength, and modulation frequency. The results perfectly correspond to the calculations based on the spin phase averaging using the cumulant expansion in the Gaussian approximation. This theory gives the spin-echo signal of confined spins as (*6, 7, 10*)

$$E(2\tau) = \sum_{j,\mathbf{k}} E_{0j}S_{\mathbf{k}}(\mathbf{F}_{aj})e^{i(\mathbf{F}_{aj}-\mathbf{k})\mathbf{r}_j(0)}e^{-(1/2)\mathbf{k}^2\mathbf{R}_{gj}^2(2\tau)}. \quad [3]$$

This expression comprises the structure terms of spin dephasing in inverse space as $S_{\mathbf{k}}(\mathbf{F}_{aj})$ that are attenuated by the factor depending on the mean squared displacement $R_{gj}^2(2\tau)$ of the particle (MSD) from the jth subensemble. The wave vectors $\mathbf{k}$ are related to the allowed momentum states of confined particles. The subscript g in MSD and in other variables denotes the component along the direction of the applied gradient. A similar result is obtained in Ref. (*15*) by using the diffusion propagator method. Both results differ in the definition of $\mathbf{F}_a$ and R_g^2. They are identical in the limit of short intervals when MSD is approximated as $R_g^2(2\tau) \approx 2D2\tau$ and when a sequence with the short gradient pulses gives $\mathbf{F}_a = \gamma\mathbf{G}\delta$. However, the generalized form of MSD is given by

$$R_{gj}^2(2\tau) = \int_0^{2\tau}\int_0^{2\tau}\langle \mathbf{v}_{gj}(t_1)\mathbf{v}_{gj}(t_2)\rangle dt_1 dt_2. \quad [4]$$

Here the VCF, $\langle \mathbf{v}_{gj}(t_1)\mathbf{v}_{gj}(t_2)\rangle$, contains the microscopic details of molecular motion in a confined space. Clearly, VCF depends on the duration of the measurement as well as on the location of the jth spin subensemble. The phasing factor $\mathbf{F}_{aj}$ (*10*) represents the average dephasing of a spin in the jth subensemble, which is, in generalized form,

$$\mathbf{F}_{aj} = \frac{\mathbf{f}\sqrt{\int_0^{2\tau}dt_1\int_0^{2\tau}dt_2\mathbf{F}(t_1)\cdot\langle\mathbf{v}_{gj}(t_1)\mathbf{v}_{gj}(t_2)\rangle\cdot\mathbf{F}(t_2)}}{R_{gj}(2\tau)}. \quad [5]$$

The unit vector $\mathbf{f}$ is aligned along the direction of the applied gradient.

The stochastic process of spin location $\mathbf{r}(t)$, which is derived from an underlying process of the velocity fluctuations $\mathbf{v}(t)$, is not in general Markovian, but acquires the Markovian character after some information is lost by limiting the precision of spatial and temporal measurements. Thus the conditional probability coincides with Fick's diffusion equation for the values of t much larger than the correlation time of molecular collisions τ_c (Einstein's approximation) and for the spatial resolution limited to a scale larger than the molecular mean free path l. The resulting conditional probability $P_o(\mathbf{r}, t|\mathbf{r}_o)$, which is commonly used to get the spin phase average for short gradient pulses, is related to VCF in the form

$$\langle \mathbf{v}_j(t_1)\mathbf{v}_j(t_2)\rangle = 2D\begin{pmatrix}1&0&0\\0&1&0\\0&0&1\end{pmatrix}\delta(t_1 - t_2). \quad [6]$$

Here D denotes the macroscopic self-diffusion constant. It simplifies Eqs. [4] and [5] to

$$R_{gj}(2\tau) = \sqrt{2D2\tau} \quad [7]$$

and

$$\mathbf{F}_{aj} = \mathbf{f}\sqrt{\frac{1}{2\tau}\int_0^{2\tau} |\mathbf{F}(t_1)|^2 dt_1}. \quad [8]$$

Thus, the cumulant expansion in the Gaussian approximation provides an identical result as the propagator method, but it allows one to apply any kind of gradient pulse sequence. The gradient pulse width or shape can violate the short pulse approximation required for the use of the propagator method.

This means that Einstein's approximation (or Fick's propagator method) can be used for restricted diffusion only when the spin-echo sequence is short enough that a majority of spin-bearing particles do not reach the compartment boundaries. The delta function is a reasonable approximation for the VCF when the rate of intermolecular collisions is much higher than the rate of collisions with the walls, $\tau_c \ll 2\tau \ll \tau_w$. This means that a better approximation for the VCF is needed for longer times, when $2\tau \approx \tau_w$. It can be solved by using the probability distribution function from Fick's equation $P_o(\mathbf{r}, t|\mathbf{r}_o)$ to calculate MSD according to the formula

$$R_g^2(t, \mathbf{r}) = \int_V (\mathbf{r} - \mathbf{r}_o)^2 P_o(\mathbf{r}, t|\mathbf{r}_o) d^3\mathbf{r}_o. \quad [9]$$

Its second time derivative provides VCF, which is needed to get the phase factor $\mathbf{F}_a(r)$ from Eq. [5].

In the following, we deal with the spatial distribution of the spin-echo signal. Therefore, we have to extend the formula for the mean spin response from the bulk of sample Eq. [3] to the formula for the spatial distribution of the spin response. In order to neglect the effect of the gradient to attenuation in the readout interval, we assume the data acquisition interval, $\delta\tau$, short compared to the inverse rate of the diffusion attenuation, $\delta\tau \ll 1/F_a^2 D$. Then the spatial distribution of the spin-echo signal, induced by the jth subensemble of spins located around $\mathbf{r}$, can be written as

$$\delta E(2\tau, \mathbf{r}) = E_0(\mathbf{r}) \sum_{\mathbf{k}} S_{\mathbf{k}}(\mathbf{F}_a(\mathbf{r})) e^{i(\mathbf{F}_a(\mathbf{r}) - \mathbf{k})\cdot\mathbf{r}} e^{-(1/2)\mathbf{k}^2 R_g^2(2\tau,\mathbf{r})}. \quad [10]$$

Attention is focused on the diffusion of molecules inside a closed pore with perfectly reflecting walls. For the sake of simplicity, we deal with one-dimensional problem, with spin-bearing particles trapped between parallel planes $x = 0$ and $x = a$, and with gradient applied normal to the planes. In this case the MSD of a spin located at x in the direction of the applied gradient is (*36*)

$$\begin{aligned} R_g^2(t, x) &= \frac{1}{a}\int_0^a (x' - x)^2 P_o(x', t|x) dx' \\ &= \frac{1}{3}(a^2 - 3ax + 3x^2) \\ &\quad + \sum_{n=1}^{\infty} \frac{4a(x + (a - x)(-1)^n)}{n^2\pi^2} \\ &\quad \times \cos\left[\frac{n\pi}{a}x\right] e^{-(n^2\pi^2/a^2)Dt} \end{aligned} \quad [11]$$

and the VCF in the second approximation is

$$\begin{aligned} \langle v_{gj}(t) v_{gj}(0)\rangle &= \frac{1}{2}\frac{d^2}{dt^2} R_g^2(t, x_j) \\ &= 2D\left(\delta(t) + \frac{D}{a^3}\sum_{n=1}^{\infty}(x_j + (a - x_j)(-1)^n)\right. \\ &\quad \left. \times n^2\pi^2 \cos\left[\frac{n\pi}{a}x_j\right] e^{-(n^2\pi^2/a^2)Dt}\right). \end{aligned} \quad [12]$$

In addition to the short correlation of the local stochastic motion, VCF features a long negative time-tail with the decay time proportional to the time-of-flight across the pore, $\tau_w \approx a^2/D$. The average of VCF over the pore volume is

$$\overline{\langle v_g(t) v_g(0)\rangle} = 2D\left(\delta(t) - \frac{4D}{a^2}\sum_{k=1}^{\infty} e^{-((2k-1)^2\pi^2/a^2)Dt}\right). \quad [13]$$

This result is identical to the solution of the Langevin equation for particles confined between parallel planes that was obtained by Oppenheim and Mazur (*2*) long ago. The simulation of molecular motion in a system constrained by capillary walls gives, on hydrodynamic grounds, a similar negative decay in algebraic form (*37*). Recently, it has been verified experimentally by the method of modulated gradient spin echo (*25*).

For the diffusion between parallel planes, the spin-echo amplitude exhibits the spatial distribution

$$\delta E(2\tau, x) = \left| \sum_{n=0}^{\infty} S_n(F_a(x)) \cos\left[\frac{n\pi}{a} x\right] \times e^{-(1/2)(n^2\pi^2/a^2) R_g^2(2\tau, x)} \right|, \quad [14]$$

with

$$S_n(F_a) = 2iF_a(x) \frac{1 - (-1)^n e^{-iF_a(x)a}}{n^2\pi^2 - F_a^2(x)a^2} \quad [15]$$

for $n > 0$ and

$$S_0(F_a(x)) = \frac{1 - e^{-iF_a(x)a}}{iF_a(x)a^2}. \quad [16]$$

These formulas will be used to compare the spin-echo distribution in a pore to the results of the numerical simulation.

3. SIMULATION

The validity of theoretical models has been tested by the computer simulation of the Brownian motion in a restricted space. Instead of considering the mean spin response from the bulk of sample, the simulation has been focused on the spatial distribution of the spin-echo signal within two parallel reflecting planes.

A common way to simulate self-diffusion is to represent the diffusion as a random walk of particles. The particle motion is represented as a sequence of small random displacements,

$$x(t + \Delta t) = x(t) + \Delta x, \quad [17]$$

where $x(t)$ is the position of the particle at time t, $x(t + \Delta t)$ is the position at time $t + \Delta t$, and Δx is a random displacement of the particle in the time interval Δt. Stochastic properties of the random displacement are associated with stochastic properties of a Brownian particle. The position of a free Brownian particle may be treated as a Markov process on a coarse time scale. In one dimension the Brownian particle jumps back and forth along the x-axis. Jumps may have any length. The probability is symmetrical and independent of the starting position and falls off rapidly for large jumps. Stochastic properties of the particle displacement Δx in the time interval Δt ($\Delta t \to 0$) are

$$\frac{\langle \Delta x \rangle}{\Delta t} = 0, \quad \frac{\langle (\Delta x)^2 \rangle}{\Delta t} = 2\mathrm{D}, \quad \frac{\langle (\Delta x)^n \rangle}{\Delta t} = 0, \quad [18]$$

where D is the macroscopic self-diffusion constant. Microscopic random displacements of the particle are the result of collisions with surrounding particles and are associated with the constant D. The Brownian particle obeys Fick's diffusion law $\dot{P} = D\nabla^2 P$. $P(x, t)$ is the probability density that a particle moves by x in time t. The well-known solution for the special case of unrestricted Brownian motion with the initial condition $P(x, 0) = \delta(x)$ is

$$P(x, t) = \frac{1}{\sqrt{4\pi D t}} e^{-(x^2/4Dt)}. \quad [19]$$

This is the Gaussian function with its maximum at the origin and whose width grows with a square root of time $\sqrt{\langle x^2(t) \rangle} = \sqrt{2Dt}$.

The random walk displacement, Δx, is therefore given by

$$\Delta x = \sqrt{2D\Delta t}\xi, \quad [20]$$

where ξ is a random number. The random numbers are uncorrelated and they are distributed according to the Gaussian distribution with $\sigma = 1$,

$$P(\xi) = \frac{1}{\sqrt{2\pi}} e^{-(\xi^2/2)}. \quad [21]$$

For a restricted space the particle trajectory is obtained by using Eqs. [17] and [20] and corrected with the boundary condition. For perfectly reflecting walls located at $x = 0$ and $x = a$, the reflecting boundary condition is accounted for by replacing x with $-x$, or x with $2a - x$, whenever $x < 0$ or $x > a$, respectively. We are dealing with a pulse sequence with two gradient pulses of strength G and duration δ, separated by time Δ. The gradient is perpendicular to the plane boundaries. The simulated spin phase shift for a single spin i is given by

$$\theta_i(2\tau) = \theta_i = \gamma G \Delta t \left(\sum_{t=0}^{t \le \delta} x_i(t) - \sum_{t=\Delta}^{t \le \Delta + \delta} x_i(t) \right). \quad [22]$$

Since the particle position randomly varies with time, the accumulated phase shift is different for every trajectory. To calculate the spin-echo distribution, we divide the space attainable to spins into N_x equal parts of length $\Delta a = a/N_x$. N_x thus represents the number of pixels in the image and Δa is the spatial resolution. Spin-echo δE of the spins located in Δa at x, at the time 2τ of the spin-echo peak, is given by

$$\delta E(x, 2\tau) = \frac{N_x}{N} \sqrt{\left(\sum_{i \in I} \cos \theta_i\right)^2 + \left(\sum_{i \in I} \sin \theta_i\right)^2}, \quad [23]$$

where I is the set of all trajectories ending within Δa at x in time 2τ: $I = \{i;\ x_i(2\tau) \in [x, x + \Delta a)\}$.

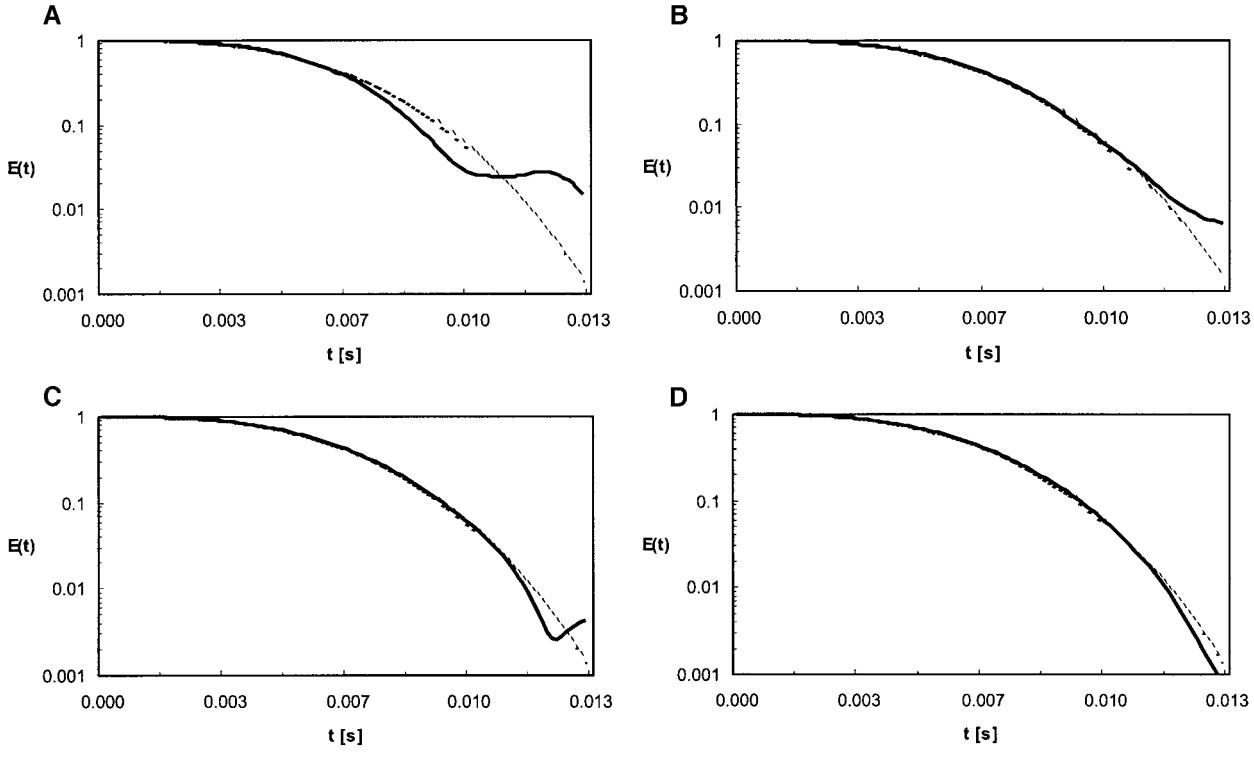

FIG. 2. Simulated signal for free self-diffusion as a function of time $t = 2\tau$ for the PGSE measurement, where $\Delta \approx \delta$ and $\tau \approx \Delta$. System parameters are the following: $D = 2 \cdot 10^{-9}$ m^2/s, $G = 0.5$ T/m, $t = 2\tau = 0$–13 ms. Simulation results are represented with a solid line. The dashed line represents the theoretical results for free self-diffusion. Simulation parameter is a number of simulated trajectories (particles). Signal from image A is obtained by simulating $N = 10^3$ trajectories. For image B, 10^4 trajectories are simulated; 10^5 and 10^6 trajectories are used for simulation results on images C and D.

The signal is obtained by simulating N spin trajectories within compartment of the size a, with uniformly distributed starting positions.

To test the computer simulation, we have first simulated the case of free self-diffusion. The spin-echo E signal from the bulk of sample is given by

$$E(2\tau) = \frac{1}{N}\sqrt{\left(\sum_{i=1}^{N}\cos\theta_i\right)^2 + \left(\sum_{i=1}^{N}\sin\theta_i\right)^2}. \qquad [24]$$

Figure 2 shows the simulated spin-echo signal as a function of time 2τ in comparison to the theoretical signal for a PGSE measurement of free self-diffusion. The deviation of the simulated results from the theoretical values can be sufficiently reduced by simulating 10^5–10^6 trajectories. As we can see, this approach assures enough accuracy for the spin-echo signal larger than 0.01. Since Monte Carlo methods by nature converge asymptotically slowly, other methods of simulation should be used (for example see (*27*)) if higher accuracy is required.

The second test of the computer simulation was the comparison of the spin-echo signal attenuation from the bulk of sample for restricted self-diffusion with the results of Callaghan and colleagues (*15*, *17*, *38*). The comparison shows very good agreement inside the range of the spin-echo signal larger than 0.01. The solid line in Fig. 3 shows the simulated signal that can be compared with Fig. 3 in (*15*). The dashed curve in Fig. 3 shows the result based on the short gradient pulse (SGP) theoretical prediction. In fact, this theory does not apply here because the gradient pulses used in the simulation are relatively long ($\delta = \Delta/4$ in Fig. 3A and $\delta = \Delta$ in Fig. 3B).

4. RESULTS AND DISCUSSION

In Figs. 4 and 5 the results of the numerical simulation of the spin-echo spatial distribution are compared with the theoretical prediction based on Fick's diffusion law, where VCF is a delta function. In Fig. 6 the simulation is compared to the attenuation obtained with use of the spatially and temporary dependent VCF for the restricted diffusion according to Eqs. [11] and [12]. The results of theory are also compared with the experimentally obtained spin-echo distribution from the MRI edge enhancement measurements, when the particle displacements were shorter than the size of pore. These results correspond to the PGSE sequence where $\Delta \approx \delta$, and $\tau \approx \Delta$. To generalize the discussion we introduce nondimensional variables for diffusion length $\tilde{L} = L/a = \sqrt{2D2\tau}/a$ and average dephasing factor

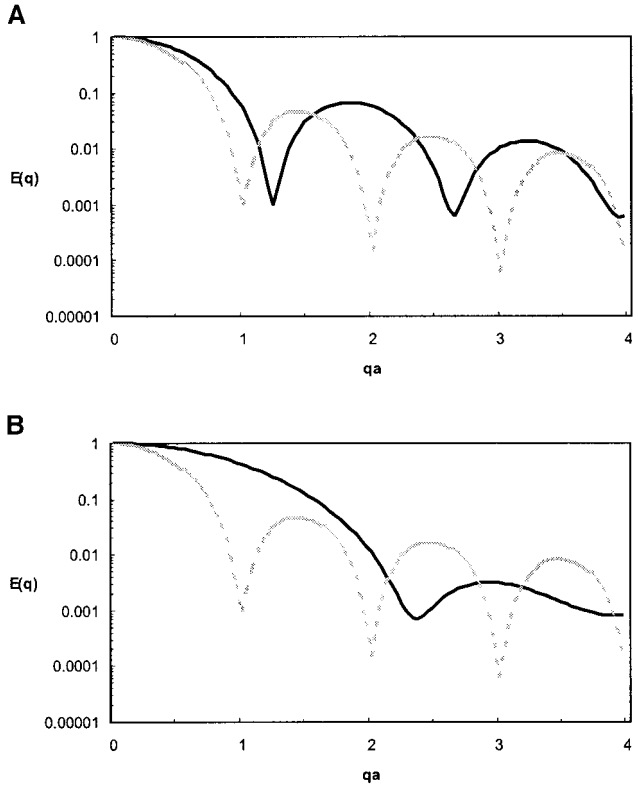

FIG. 3. Simulated PGSE signal for the case of restricted self-diffusion between parallel planes separated by a, as a function of product $qa = (2\pi)^{-1}\gamma G\delta a$. Walls are perfectly reflecting. System parameters are the following: $\Delta = 0.6a^2/D$, image A: $\delta = \Delta/4$, image B: $\delta = \Delta$. Signal was obtained by simulating $N = 10^6$ trajectories. The solid line shows simulated results and the dashed curve shows for reference the theoretical attenuation for the short gradient pulse limit.

$\tilde{F}_a = F_a a$. The discussion is divided into three parts. The comparison between the simulated and theoretical results of the spin-echo spatial distributions is performed for short diffusion times ($\tilde{L} < 0.1$) in the first part and for larger diffusion times ($\tilde{L} > 0.5$) in the second part. While in the third part, the results of simulation are compared with the experimental results of MRI edge enhancement.

4.1. Short Diffusion Times

When the duration of a PGSE sequence is short enough that only the minority of spin-bearing particles collides with the boundary, the molecules exhibit almost the same dynamics as in the case of free self-diffusion. In this approximation the spin-echo distribution in a pore from Eq. [14] is calculated with the use of Eq. [7] for MSD and Eq. [8] for the phasing factor. The results provide a good fit to the results of numerical simulation, as seen in Fig. 4. It confirms, on an empirical basis, that this zeroth approximation works well, as long as the diffusion displacement is short ($\tilde{L} < 0.1$). The agreement between Einstein's approximation of VCF and the simulation is very good because the edge enhancement results mainly from the eigenvalue nature of Eqs. [14], i.e., the $\cos(n\pi x/a)$ term, while the long negative time tail of VCF has a negligible effect.

4.2. Larger Diffusion Times

Implementation of Eq. [7] for long gradient pulse causes a deviation, as shown in Fig. 5. The difference increases with the diffusion time. Curiously, the theory that seems to perfectly agree with the simulation when considering the spin response from the bulk fails when it is used for the prediction of the spatial distribution of the spin-echo signal. It indicates that VCF with the fast decay, a delta function approximation, is not appropriate when particle displacements are comparable to the size of the pore. According to Refs. (*2, 37*) and Eqs. [11] and [12], the effect of the wall is to add a small but long negative time tail to the VCF. For very long times the effect of this negative correlation essentially cancels out the effect of the initial positive collision correlation for short diffusion time. In this generalized form, the time integration in Eq. [4] provides the MSD that cannot be larger than the pore size.

Therefore, the temporally and spatially dependent VCF for reflecting walls (Eq. [12]) is needed to get the MSD in Eq. [4] and to calculate special dependence of the spin-echo attenuation. Since the spatially averaged MSD, $\tilde{R}_g^2$, approaches the asymptotic value $\sqrt{a^2/6}$ for long diffusion times, we can

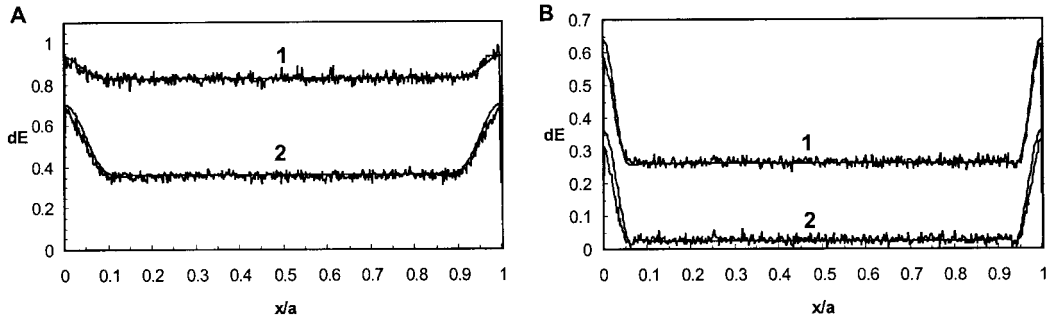

FIG. 4. Spin-echo spatial distribution for self-diffusion between parallel reflecting planes for short diffusion times ($\tilde{L} < 0.1$), predicted by simulation (jagged line) and theory, VCF approximated with a delta function, (smooth line). System parameters are the following: image A: $\tilde{L}_1 = 0.04$, $\tilde{F}_{a1} = 15.4$ and $\tilde{L}_2 = 0.052$, $\tilde{F}_{a2} = 27$, image B: $\tilde{L}_1 = 0.028$, $\tilde{F}_{a1} = 115.8$ and $\tilde{L}_2 = 0.033$, $\tilde{F}_{a2} = 162.2$. Pulse duration and pulse separation are the same for all images: $\Delta \approx \delta$ and $\tau \approx \Delta$.

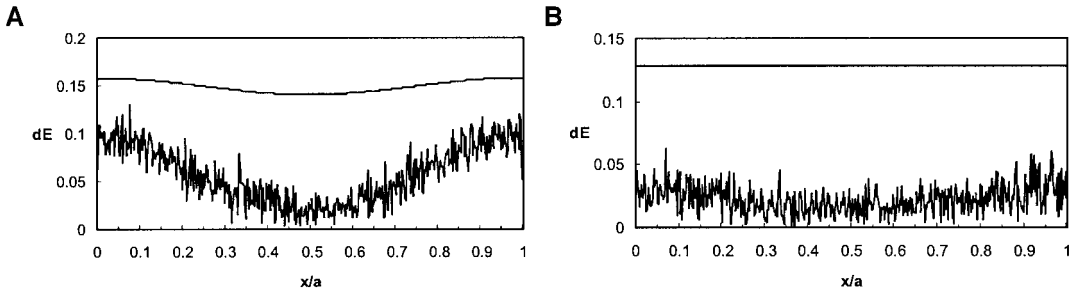

FIG. 5. Spin-echo spatial distribution for self-diffusion between parallel reflecting planes for intermediate and long diffusion times ($\tilde{L} \approx 0.5$ and $\tilde{L} > 0.5$), respectively, and predicted by simulation (jagged line) and theory, VCF approximated with a delta function (smooth line). System parameters are the following: image A: $\tilde{L} = 0.52$, $\tilde{F}_a = 21.6$, image B: $\tilde{L} = 0.63$, $\tilde{F}_a = 30.9$. Pulse duration and pulse separation are the same for all images: $\Delta \approx \delta$ and $\tau \approx \Delta$.

distinguish between the diffusion displacement R_g which has an upper limit and the diffusion length L, calculated as the diffusion displacement in the free self-diffusion case. The diffusion displacement stands for the average distance between the starting and the current position of the particle, while L represents the averaged length of the forth-and-back traveling.

The spin dephasing F_a was calculated by using a VCF averaged over the space of confinement, Eq. [13] as obtained in Ref. (*2*), thus, ignoring the spatial dependence in expression [5]. The spatial dependence of VCF was taken into account only for the MSD, Eq. [4]. With these modifications, the calculated spatial distribution of attenuation from Eq. [14] in Fig. 6 shows a better fit Fig. 5 for intermediate displacements, $\tilde{L} \approx 0.5$. For larger displacements, $\tilde{L} > 0.5$, the theoretical attenuation is again too weak compare to the results of simulation. This departure might be caused either by the neglect of the spatial dependence of VCF in the dephasing term Eq. [5] or by the insufficiency of the Gaussian approximation for long diffusion displacements inside entirely closed pores. Cumulants higher then the second might not be negligible. In contrast to this, Eq. [3] perfectly explains the measurements of self-diffusion attenuation in a medium of interconnected pores (*25*). This might indicate an importance of medium permeability when using the Gaussian approximation for NMR of restricted diffusion.

4.3. Experimental Results

The experimental results are available from the MRI edge enhancement in the compartment where the diffusion displacements were much shorter than the wall interspacing. This results have already been published (*10*). Here we compare the intensities of enhanced edges and the intensity of the middle part of the image with the results of numerical simulation. A simulated and theoretical log–log plot of the signal in Fig. 8 as a function of time exhibits a good agreement with the experiment, Fig. 7. According to slopes, the attenuation of bulk signal increases as τ^3. A deviation from this law on the MR image is due to the experimental error. The lines of enhanced edges in both cases follow almost a linear dependence on the diffusion time. This agrees with the theory, where the line broadening, which is proportional to MSD, $R_g^2 = 2D2\tau$, lowers the intensity of enhanced lines in proportion.

5. CONCLUSION

In this analysis, the numerical simulation of the spin-echo attenuation with finite-width gradient pulses was used to test various approximations of velocity correlation function when diffusion in the closed pore is considered. Comparison of simulation results with the theoretical evaluation and the ex-

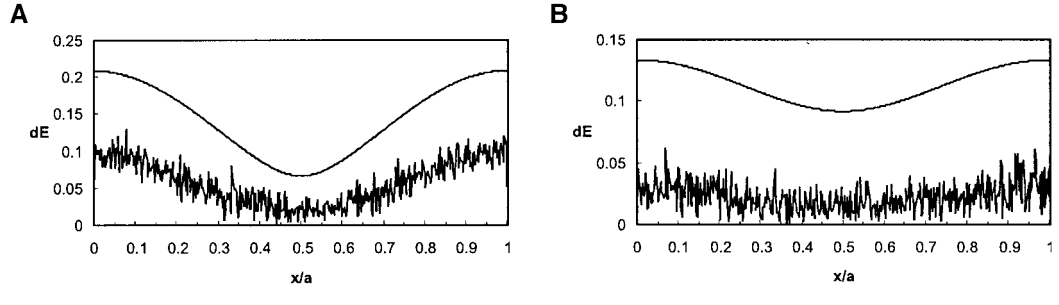

FIG. 6. Spin-echo spatial distribution for the case of diffusion displacements between parallel and reflecting walls for intermediate and long diffusion times ($\tilde{L} \approx 0.5$ and $\tilde{L} > 0.5$), respectively, predicted by simulation (jagged line) and theory accounting for the spatially dependent modified Oppenheim–Mazur VCF (smooth line). System parameters are the following: image A: $\tilde{L} = 0.52$, $\tilde{F}_a = 21.6$, image B: $\tilde{L} = 0.63$, $\tilde{F}_a = 30.9$. Pulse duration and pulse separation are the same for all images: $\Delta \approx \delta$ and $\tau \approx \Delta$.

perimental results of MRI edge enhancement is focused on the distribution of spin-echo signal within the confinement. The simulation studies hitherto considered the signal from the bulk of the sample while the present analysis is focused on the spatial distribution of the signal to get a detailed insight into the occurrence in the proximity of the walls. For VCF in Einstein's approximation (delta function), the attenuation distribution obtained by the cumulant expansion in the Gaussian approximation gives a good fit to the results of the simulation (Fig. 4) for the mean squared displacement short compared to the size of the compartment, ($\tilde{L} < 0.1$). Clearly, at short times, the edge enhancement is only due to the boundary conditions and the eigenvalue nature of Eqs. [10] and [14], while the long negative time tail of VCF can be neglected. However, this approximation deviates strongly from the result of simulation (Fig. 5) when the number of spins collisions on walls increases ($\tilde{L} > 0.1$). Curiously, the theory of short gradient pulses, which perfectly agrees with the simulation when the entire spin response is considered, fails to give the proper spatial distribution for the MSD larger than a few tenths of the pore size. Therefore, Fick's diffusion law is just a first approximation that has to be complemented with the details of motional correlation in the confinement. For large diffusion displacements, we are seeing interplay of the correlation dynamics and the boundary conditions, so that a complete analysis requires the knowledge of the MSD as well as the VCF dependence on the distance from the wall. The Oppenheim–Mazur solution of the Langevin equation, which provides the VCF averaged over the space of confinement (*2*), is used to calculate an averaged spin dephasing F_a, thus ignoring a spatial dependence in Eq. [5]. The spatial dependence was taken into account only for the MSD, Eq. [4]. The results provide a good fit to the numerically obtained dependence at least for an intermediate MSD, ($\tilde{L} \leq 0.5$). This confirms the profound effect of the correlation, particularly in a medium with small pores. However, the deviation for long displacement ($\tilde{L} > 0.5$) also indicates a deficiency of the Gaussian approximation. Although the experiment proves a sufficiency of the Gaussian approximation for the spin-echo attenuation in interconnected pores (*25*), this study implies a need either to account for cumulants higher than the second one or to take into account spatial dependence of spin dephasing, in the case of large displacements inside entirely closed pores. Callaghan and Codd have used the impulse propagator method to simulate MRI edge enhancement (*9*). The method generates the *k*-space data for the profile and Fourier transforming to get the spatial spin density. This method provides similar spatial intensity plots as our simulated results (Figs. 4 and 6). However, it also generates a spectral distortion that unreality broadens the image far beyond the edge of the sample. It is not the case with our method of simulation.

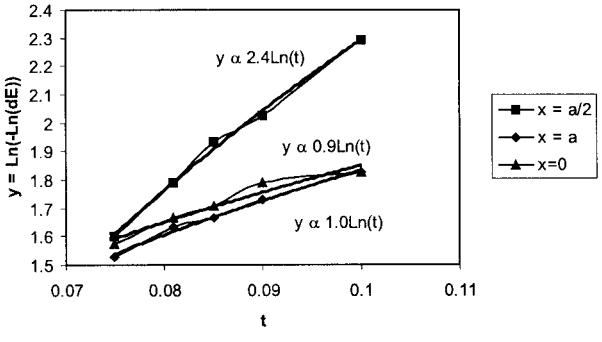

FIG. 7. Intensities of three sections of a one-dimensional experimental MR image as a function of time of the spin-echo in logarithmic scale ($G = 0.03$ T/m, $a = 2.8$ mm, $D = 2 \cdot 10^{-9}$ m^2/s). The signal of the bulk spin-echo ($x = a/2$) decreases with $E(t) \propto e^{-\beta t^3}$ and the lines of enhanced edges ($x = 0, a$) follow almost $E(t) \propto e^{-\beta t}$.

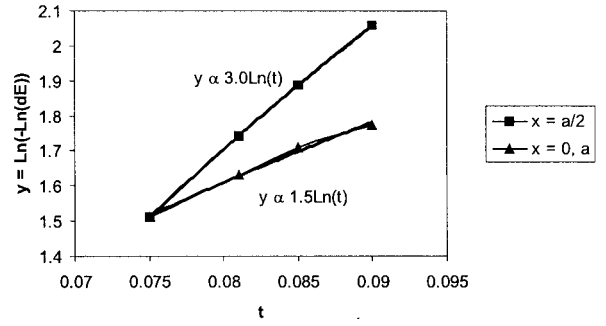

FIG. 8. Intensities of various sections of a one-dimensional theoretical and simulated MR image as a function of time of the spin-echo in logarithmic scale ($G = 0.03$ T/m, $a = 2.8$ mm, $D = 2 \cdot 10^{-9}$ m^2/s). The signal of the bulk spin-echo ($x = a/2$) decreases with $E(t) \propto e^{-\beta t^3}$ and the lines of enhanced edges ($x = 0, a$) follow $E(t) \propto e^{-\beta t^{1.5}}$.

REFERENCES

1. P. T. Callaghan, "Principles of Nuclear Magnetic Resonance Microscopy," Oxford Univ. Press, Oxford, 1991.
2. E. Oppenheim and P. Mazur, Brownian motion in system of finite size. *Physica* **30,** 1833–1845 (1964).
3. J. Kärger and W. Heink, The propagator representation of molecular transport in microporous crystallites. *J. Magn. Reson.* **51,** 1–7 (1983).
4. P. T. Callaghan, C. D. Eccles, and Y. Xia, NMR microscopy of dynamic displacements: k-space and q-space imaging. *J. Phys. E* **21,** 820–822 (1988).
5. C. H. Neuman, Spin echo of spins diffusing in a bounded medium. *J. Chem. Phys.* **60,** 4508–4511 (1974).
6. J. Stepišnik, Spin echo attenuation of restricted diffusion as a discord of spin phase structure. *J. Magn. Reson.* **131,** 339–346 (1998).
7. J. Stepišnik, Validity limits of gaussian approximation in cumulant expansion for diffusion attenuation of spin echo. *Phys. B* **270,** 110–117 (1999).
8. L. Z. Wang, A. Caprihan, and E. Fukushima, The narrow-pulse criterion for pulsed-gradient spin echo diffusion measurement. *J. Magn. Reson. A* **117,** 209–219 (1995).
9. P. T. Callaghan and S. L. Codd, Generalised calculation of NMR imaging edge effects arising from restricted diffusion in porous media. *Magn. Reson. Imaging* **16,** 471–478 (1998).

10. J. Stepišnik, A. Duh, A. Mohorič, and I. Serša, MRI edge enhancement as a diffusive discord of spin phase structure. *J. Magn. Reson.* **137,** 154–160 (1999).
11. E. L. Hahn, Spin-echoes. *Phys. Rev.* **80,** 580–594 (1950).
12. H. C. Torrey, Transient nutations in nuclear magnetic resonance. *Phys. Rev.* **76,** 1095–1068 (1946).
13. E. O. Stejskal and J. E. Tanner, Spin diffusion measurements: Spin-echoes in the presence of a time-dependent field gradient. *J. Chem. Phys.* **42,** 288–292 (1995).
14. Albert Einstein, "Investigation on the Theory of the Brownian Movement," Academic Press, New York, 1956.
15. A. Coy and P. T. Callaghan, Pulsed gradient spin echo nuclear magnetic resonance for molecules diffusing between partially reflecting rectangular barriers. *J. Chem. Phys.* **101,** 4599–4609 (1994).
16. A. Caphrihan, L. Z. Wang, and E. Fukushima, A multiple-narrow-pulse approximation for restricted diffusion in a time-varying field gradient. *J. Magn. Reson. A* **118,** 94–102 (1996).
17. P. T. Callaghan, A simple matrix formalism for spin echo analysis of restricted diffusion under generalized gradient waveforms. *J. Magn. Reson.* **129,** 74–84 (1997).
18. R. Kubo, "Some aspects of the statistical–mechanical theory of irreversible processes, *in* "Lectures on Theoretical Physics," Interscience, New York, 1959.
19. J. Stepišnik, Analysis of nmr self-diffusion measurements by density matrix calculation. *Phys. B* **104,** 350–364 (1981).
20. J. Stepišnik, Measuring and imaging of flow by NMR. *Progr. NMR Spectrosc.* **17,** 187–209 (1985).
21. J. Stepišnik, NMR measurement and Brownian movement in the short-time limit. *Phys. B* **198,** 299–306 (1994).
22. J. Stepišnik, M. Kos, G. Planinšič, and V. Eržen, Strong nonuniform magnetic field for a self-diffusion measurement by NMR in the earth's magnetic. *J. Magn. Reson. A* **107,** 167–172 (1994).
23. P. T. Callaghan and J. Stepišnik, Frequency-domain analysis of spin motion using modulated gradient nmr. *J. Magn. Reson. A* **117,** 118–122 (1995).
24. P. T. Callaghan and J. Stepišnik, Generalised analysis of motion using magnetic field gradients, *in* "Advances in Magnetic and Optical Resonance" (Waren S. Warren, Ed.), Vol. 19, pp. 326–389, Academic Press, San Diego, 1996.
25. J. Stepišnik and P. T. Callaghan, The long time-tail of molecular velocity correlation in a confined fluid: Observation by modulated gradient spin echo nmr. *Phys. B* **292,** 296–301 (2000).
26. B. Balinov, B. Jönsson, P. Linse, and O. Söderman, The NMR self-diffusion method applied to restricted diffusion. Simulation of echo attenuation from molecules in spheres and between planes. *J. Magn. Reson. A* **104,** 17–25 (1993).
27. M. H. Blees, The effect of finite duration of gradient pulses on the pulsed-field-gradient NMR method for studying restricted diffusion. *J. Magn. Reson. A* **109,** 203–209 (1994).
28. B. Putz, D. Barsky, and K. Schulten, Edge enhancement by diffusion in microscopic magnetic resonance imaging. *J. Magn. Reson. A* **976,** 27–53 (1992).
29. P. T. Callaghan, A. Coy, L. C. Forde, and C. J. Rofe, Diffusive relaxation and edge enhancement in NMR microscopy. *J. Magn. Reson. A* **101,** 347–350 (1993).
30. T. M. de Swiet, Diffusive edge enhancement in imaging. *J. Magn. Reson. B* **109,** 12–18 (1995).
31. B. Saam, N. Drukker, and W. Happer, Edge enhancement observed with hyperpolarized ^{3}He. *Chem. Phys. Lett.* **263,** 481–487 (1996).
32. Yi-Qiao Song, B. M. Goodson, B. Sheridan, T. M. de Swiet, and A. Pines, Effects of diffusion on magnetic resonance imaging of laser-polarized xenon gas. *J. Chem. Phys.* **108,** 6233–6239 (1998).
33. G. Arfken, "Mathematical Methods for Physicists," Academic Press, New York, 1970.
34. N. G. van Kampen, "Stochastic Processes in Physics and Chemistry," North-Holland, Amsterdam, 1981.
35. R. Kubo, M. Toda, and N. Hashitsume, "Statistical Physics II: Nonequilibrium Statistical Mechanics," Springer-Verlag, Germany, 1991.
36. A. Duh, "Restricted Self-Diffusion and Edge Enhancement at NMR Microscopy," Thesis, University of Ljubljana, 1999.
37. M. H. J. Hagen, I. Pagonabarraga, C. P. Lowe, and D. Frenkel, Algebraic decay of velocity fluctuations in a confined fluid. *Phys. Rev. Lett.* **78,** 3785–3788 (1997).
38. S. L. Codd and P. T. Callaghan, Spin echo analysis of restricted diffusion under generalized gradient waveforms: Planar, cylindrical, and spherical pores with wall relaxivity. *J. Magn. Reson.* **137,** 358–372 (1999).